# Sphingosine 1-phosphate induces cytoskeletal reorganization in C2C12 myoblasts: physiological relevance for stress fibres in the modulation of ion current through stretch-activated channels

**Lucia Formigli[1], Elisabetta Meacci[2], Chiasa Sassoli[1], Flaminia Chellini[1], Rosalba Giannini[1], Franco Quercioli[3], Bruno Tiribilli[3], Roberta Squecco[4], Paola Bruni[2], Fabio Francini[4] and Sandra Zecchi-Orlandini[1,*]**

Departments of [1]Anatomy, Histology and Forensic Medicine, [2]Biochemical Sciences, [3]National Institute of Applied Optics and [4]Department of Physiological Sciences, Interuniversitary Institute of Miology (IIM), 85 50134 Florence, Italy

*Author for correspondence (e-mail: zecchi@unifi.it)

*Accepted 30 December 2004*
*Journal of Cell Science 118, 1161-1171 Published by The Company of Biologists 2005*
*doi:10.1242/jcs.01695*

## Summary

**Sphingosine 1-phosphate (S1P) is a bioactive lipid that is abundantly present in the serum and mediates multiple biological responses. With the aim of extending our knowledge on the role played by S1P in the regulation of cytoskeletal reorganization, native as well as C2C12 myoblasts stably transfected with green fluorescent protein (GFP)-tagged α- and β-actin constructs were stimulated with S1P (1 μM) and observed under confocal and multiphoton microscopes. The addition of S1P induced the appearance of actin stress fibres and focal adhesions through Rho- and phospholipase D (PLD)-mediated pathways. The cytoskeletal response was dependent on the extracellular action of S1P through its specific surface receptors, since the intracellular delivery of the sphingolipid by microinjection was unable to modify the actin cytoskeletal assembly. Interestingly, it was revealed by whole-cell patch-clamp that S1P-induced stress fibre formation was associated with increased ion currents and conductance through stretch-activated channels (SACs), thereby suggesting a possible regulatory role for organized actin in channel sensitivity. Experiments aimed at stretching the plasma membrane of C2C12 cells, using the cantilever of an atomic force microscope, indicated that there was a $Ca^{2+}$ influx through putative SACs. In conclusion, the present data suggest novel mechanisms of S1P signalling involving actin cytoskeletal reorganization and $Ca^{2+}$ elevation through SACs that might influence myoblastic functions.**

Key words: S1P, Myoblast, Cytoskeleton, Stretch-activated channel, SAC, Rho pathway, PLD pathway

## Introduction

Substantial work has been carried out in the past decade to identify signalling networks that control the organization of the actin cytoskeleton, thus providing the basis for the understanding of several essential cell processes, including cell adhesion, spreading and migration. These events are mainly dependent on the activation of G-protein-coupled receptors (GPCRs) and require the engagement of members of the Rho family of small guanosine triphosphatase (GTPase) proteins which, acting as downstream molecular switches, affect the assembly and disassembly of filamentous actin (F-actin) (Hall, 1998; Seasholtz et al., 1999). The best-characterized members of this family are RhoA, Rac1 and Cdc42, whose functions have been related to distinct patterns of cytoskeletal reorganization. For instance, RhoA stimulates the organization of actin filaments into stress fibres and the recruitment of focal adhesion proteins, whereas Rac1 and Cdc42 regulate cell polarity by directing peripheral actin polymerization and the formation of lamellipodia and filopodia extensions, respectively. It is now becoming clear that Rho proteins are not simply regulators of actin-containing structures, but they may also positively regulate gene transcription (Takano et al., 1998; Ridley, 2001), possibly through the structural reorganization of the cytoskeleton (Mack et al., 2001; Hubchak et al., 2003). In particular, the activation of serum response factor, which controls transcription of many serum-inducible and muscle-specific genes, is associated with Rho-dependent changes in actin polymerization (Sotiropoulus et al., 1999; Arai et al., 2002). Moreover, many signalling molecules may be activated upon focal adhesion assembly, including those within the mitogen-activated protein kinase (MAPK) cascade (Van Aelst and D'Souza-Schorey, 1997; Turner, 2000).

S1P is a lysophospholipid that is released upon platelet activation and is physiologically present in plasma and serum (Pyne and Pyne, 2000). Most of its effects on target cells are mediated by GPCRs of the sphingosine 1-phosphate receptor (S1PR) family and involve the regulation of many actin-based functions, including angiogenesis, myocardial development, tumour dissemination and immune cell migration (Panetti et al., 2001; Hla, 2003). Indeed, the activation of S1PRs regulates

the reorganization of the actin cytoskeleton in different ways, ranging from the activation of Rho-dependent stress fibre/focal adhesion pathways to Rac-induced cortical actin assembly (Wang et al., 1997; Olivera et al., 2003; Shikata et al., 2003a; Shikata et al., 2003b). Moreover, stress fibre formation by S1P might also be dependent on the activation of phospholipase D (PLD) and, consistently, a direct role for this enzyme in actin bundling has been proposed (Kam and Exton, 2001; Porcelli et al., 2002). In this connection, although its physiological role has not been explored as yet, we have previously demonstrated that both PLD isoforms, PLD1 and PLD2, are expressed and activated in response to exogenous S1P in C2C12 myoblasts (Meacci et al., 1999a). Subsequently, we have shown in the same cells that the bioactive lipid is also capable of enhancing the levels of myosin light chain phosphorylation and increasing myoblastic contractility through $Ca^{2+}$-independent/Rho-dependent pathways (Formigli at al., 2002; Formigli et al., 2004). With this background, and in consideration of the role played by Rho-stimulated contractility in driving acto-myosin bundling into stress fibres (Chrzanowska-Wodnicka and Burridge, 1996), in the current study we investigated more deeply the role exerted by S1P in the regulation of cytoskeletal remodelling in myoblastic cells. The formation of stress fibres and focal contacts as well as the signalling components of the cytoskeletal response were analysed in C2C12 cells stimulated with S1P. The actin dynamics during these complex morphological changes was also investigated in living C2C12 cells stably transfected with green fluorescent protein (GFP)-tagged α- and β-actins and observed by two-photon excitation fluorescence microscopy.

Finally, to find a possible physiological correlation of S1P-induced stress fibres, we investigated whether the increased actin polymerization produced some mechanical perturbation (stretching) of the plasma membrane, thus modifying ion influx through stretch-activated cation channels (SACs). Since $Ca^{2+}$ influx is a characteristic feature of activated SACs (Munevar et al., 2004), and $Ca^{2+}$ is recognized as an important messenger for skeletal muscle differentiation (Berridge et al., 2000), we suggest that increased ion/$Ca^{2+}$ plasma membrane conductance observed in myoblasts with well-organized actin cytoskeleton may represent a novel mechanism by which S1P influences skeletal muscle physiology and development.

## Materials and Methods

### Cell cultures

C2C12 mouse skeletal myoblasts were obtained from American Type Culture Collection (Manassas) and grown in DMEM supplemented with 10% fetal calf serum, penicillin (100 U/ml) and streptomycin (100 μg/ml) (Sigma), and maintained at 37°C in a humidified atmosphere of 5% $CO_2$. Myoblasts were seeded into 60 or 100 mm diameter dishes and 80% confluent cells were shifted to DMEM without serum containing 0.1% BSA for 24 hours and utilized for the experiments. C2C12 cells stably transfected with constructs encoding GFP-tagged α- and β-actins were cultured in the same conditions as above.

### Cell transfection

To analyse actin cytoskeletal dynamics induced by S1P stimulation, C2C12 myoblasts were transfected with the mouse α- and β-actin genes. For transient transfection, the cells were grown in 100 mm-diameter tissue culture dishes containing 25 mm square glass coverslips at 80% confluence and cotransfected with 6 μg of pGFP-α-actin and 6 μg of pGFP-β-actin using Lipofectamine 2000 Reagent (Invitrogen), essentially as previously described (Hodgson et al., 2000). Expression and stability of expressed proteins were assessed by the analysis of the fluorescence of GFP after 18, 24 and 48 hours of transfection with two-photon excitation fluorescence microscopy. The fusion proteins were expressed at detectable levels 48 hours after transfection. Stable clones were selected for 4-6 weeks in 400 μg/ml Geneticin (Invitrogen) and maintained in 100 μg/ml Geneticin. To downregulate PLD activity, C2C12 myoblasts as well as GFP-actin-expressing C2C12 cells were transiently transfected with the expression vector pCGN encoding for catalytically inactive PLD1 mutant (K898R) tagged with haemoagglutinin [HA; dominant-negative PLD (DN-PLD), kindly provided by M. Frohman, Dept of Pharmacology, Stony Brook, NY]. After 24 hours of transfection, the cells were processed for western analysis and PLD activity.

### Construction of GFP-α-actin and GFP-β-actin expression vectors

Total cellular RNA was extracted from C2C12 myoblasts using TRIREAGENT (Sigma), according to the manufacturer's protocol. 1 μg RNA was reverse transcribed and amplified by PCR with the SuperScript™ One-Step RT-PCR System (Invitrogen) using the following mouse gene-specific primers: forward primer (ATGTGCG-ACGAAGACGAGAC) and reverse primer (GTGCGCCTAGAAG-CATTTGC) for the α-actin coding region; forward primer (ATG-GATGACGATATCGCTGC) and reverse primer (CTAGAAGCAC-TTGCGGTGCA) for the β-actin coding region. The resulting PCR products were separately subcloned in-frame downstream of modified cycle 3 GFP into the mammalian expression vector pcDNA3.1/NT-GFP-TOPO (Invitrogen) using the TA cloning kit (Invitrogen). Under the cytomegalovirus promoter, the constructs (pGFP-α-actin and pGFP-β-actin) expressed a full-length α- and β-actin with GFP fused to the amino terminus. *Escherichia coli* TOP10 competent cells (Invitrogen) were transformed with the plasmids. Plasmid purification was performed by QIA filter Plasmid Maxi Kit (Qiagen) according to the manufacturer's supplied protocol. The nucleotide sequences of all PCR products were confirmed by automated DNA sequencing.

### Measurement of PLD activity

PLD activity was determined by measuring [$^3$H]phosphatidylethanol [$^3$H](PtdEtOH) produced via PLD-catalysed transphosphatidylation in serum-starved vector or DN-PLD myoblasts and labelled for the last 16 hours of transfection with 5 μCi/ml [$^3$H]glycerol. [$^3$H]glycerol-labelled cells were incubated for 2 minutes before S1P addition in the presence of 2% ethanol. The incubation was arrested after 5 minutes at 37°C by removing the medium, washing the monolayers twice with ice-cold PBS and adding 1 ml of ice-cold methanol. [$^3$H]PtdEtOH formation was quantified after lipid extraction and TLC separation essentially as previously described (Meacci et al., 1999b).

### Western blot analysis

Vector- or DN-PLD-transfected myoblasts were lysed for 30 minutes at 4°C in a buffer containing 50 mM Tris, pH 7.5, 120 mM NaCl, 1 mM EDTA, 6 mM EGTA, 15 mM $Na_4P_2O_7$, 20 mM NaF, 1% Nonidet, 0.1% phenylmethyl sulfonylfluoride and protease inhibitors (0.08 μM aprotinin, 0.02 μM leupeptin, 0.04 μM bestatin and 15 μM pepstatin). To prepare total cell lysates, cell extracts were successively centrifuged for 15 minutes at 10,000 ***g*** at 4°C. Proteins (30 μg) from cell lysates were separated by SDS-PAGE. Proteins were then electrotransferred to nitrocellulose membranes, which were incubated overnight in Tris-buffered saline containing 0.1% Tween-20 (TTBS) and 1% BSA. Membranes were subsequently incubated for 1 hour with anti-HA (Sigma). Hybridization with primary antibodies was

followed by washing with TTBS and incubation with peroxidase-conjugated goat anti-mouse IgG1 (Santa Cruz Biotechnology). Proteins were detected by enhanced chemiluminescence (ECL; Amersham Bioscience).

### Treatment with inhibitors

Control as well as GFP-actin-transfected C2C12 cells were incubated with different inhibitors to assess the signalling pathways involved in S1P-mediated cytoskeletal reorganization. Following pretreatment with selective inhibitors of Rho kinase (Y-27632, 50 μM; Calbiochem), p38 MAPK (SB203580, 5 μM; Tocris) and of the ERK pathway (PD98059, 5 μM; Tocris) for 10 minutes, the cells were stimulated with S1P for 30 minutes and then fixed for cytoskeletal staining. To examine the involvement of Gi-coupled receptor in S1P-induced stress fibre formation, C2C12 cells were pretreated with 200 ng/ml pertussis toxin (PTx; List Biological Laboratories) for 16 hours prior to stimulation.

### Two-photon excitation fluorescence microscopy set-up

To avoid photobleaching and phototoxic cell damage, time-lapse 3D imaging of actin dynamics was performed with two-photon excitation fluorescence microscope. A Nikon PCM2000 (Nikon) confocal laser scanning microscope was modified to allow the use of an ultrafast laser source (Denk et al., 1990; Quercioli et al., 2004). One of the standard long-pass input excitation dichroics was replaced inside the confocal head with a suitable short-pass one with a wavelength cutoff at 650 nm (Chroma Technology). A 3 mm thick BG39 filter glass (Schott Glas) was used as the emission filter in the detection channel to assure total extinction of the excitation light while collecting all the emitted fluorescence. The inverted optical microscope was a Nikon TE2000-U and a Nikon PlanApo 60×/1.2 NA water immersion objective was used for best refracting index matching with the cell culture medium. The laser system was a modelocked Ti:Sapphire oscillator (Mira 900 F) pumped by a 5W laser at 532 nm (Verdi V5; Coherent). An excitation wavelength at 790 nm was chosen near the GFP two-photon excitation peak. The glass coverslips containing GFP-actin-transfected cells were mounted in an open chamber placed onto a 37°C heated microscope stage (Eliwell). The cells were then stimulated with S1P and visualized with the multiphoton microscope. For each time point, a stack of about 35 optical sections (190 μm × 190 μm, 512×512 pixels each) were taken through the depth of the cells at z intervals of 0.3 μm. An integrated extended-focus image was then obtained. This procedure allowed the imaging of the whole cell volume at the highest resolution of 250 nm lateral and 750 nm axial, at high contrast, without any out-of-focus blur.

### Confocal immunofluorescence

C2C12 cells grown on glass coverslips were stimulated with 1 μM S1P (Calbiochem) for different times (10, 20, 30, 45 and 60 minutes) and then fixed in 0.5% buffered paraformaldehyde for 10 minutes at room temperature. After permeabilization with cold acetone, the fixed cells were blocked with 0.5% BSA and 3% glycerol in PBS for 30 minutes and then stained with tetramethyl rhodamine-isothiocyanate (TRITC)-labelled phalloidin (1:100; Sigma) for F-actin. To detect focal adhesions, the cells were incubated with mouse monoclonal anti-vinculin antibody (1:100; Sigma) for 1 hour at room temperature, and immunorevealed with Alexa488-conjugated secondary antibodies (1:100; Molecular Probes). After washing, the coverslips containing the immunolabelled cells were mounted with an antifade mounting medium (Biomeda Gel mount, Electron Microscopy Sciences) and observed under a Bio-Rad MRC 1024 ES Confocal Laser Scanning Microscope (CLSM; Bio-Rad) equipped with a Krypton/Argon (Kr/Ar) laser source. Negative controls were carried out by replacing the primary antibody with non-immune mouse serum. The Argon (488 nm) and Krypton (568 nm) laser lines were used to excite the cells simultaneously, and the emitted fluorescence signals were collected with a Nikon PlanApo 60×/1.4 NA oil immersion objective. A series of optical sections (180 μm × 180 μm, 512×512 pixels each) were then taken through the depth of the cells at intervals of 0.8 μm. In some experiments, the immunostaining was also performed on GFP-actin-transfected cells, where vinculin immunostaining was revealed with Cy5-conjugated secondary antibody (1:100; Chemicon).

### Microinjection experiments

Different concentrations of S1P (5, 10, 500 μM) were microinjected together with propidium iodide (PI; 5 mg/ml; Molecular Probes) as tracking agent into the cytoplasm of C2C12 cells under a phase contrast microscope using a pressure injection system (Femtojet InjectMan NI2; Eppendorf). Approximately 10-20 cells were microinjected in each experiment ($n$=3). 30 minutes after microinjection, the coverslips were fixed and stained with Alexa488-conjugated phalloidin (Molecular Probes) to reveal F-actin organization. Control cells were microinjected solely with PI and then stimulated with exogenous S1P (1 μM). Observations were performed with a BioRad confocal microscope.

### Electrophysiology

The electrophysiological properties of C2C12 myoblasts were analysed by single microelectrode whole-cell patch-clamp in voltage-clamp conditions. Coverslips with the adherent cells were placed on the stage of a Nikon Eclipse TE 2000 inverted microscope (Nikon). During the experiments, the cells were superfused with a physiological bath solution containing 150 mM NaCl, 5 mM KCl, 2.5 mM $CaCl_2$, 1 mM $MgCl_2$, 10 mM D-glucose and 10 mM HEPES. The patch pipettes were filled with a solution containing 150 mM CsBr, 5

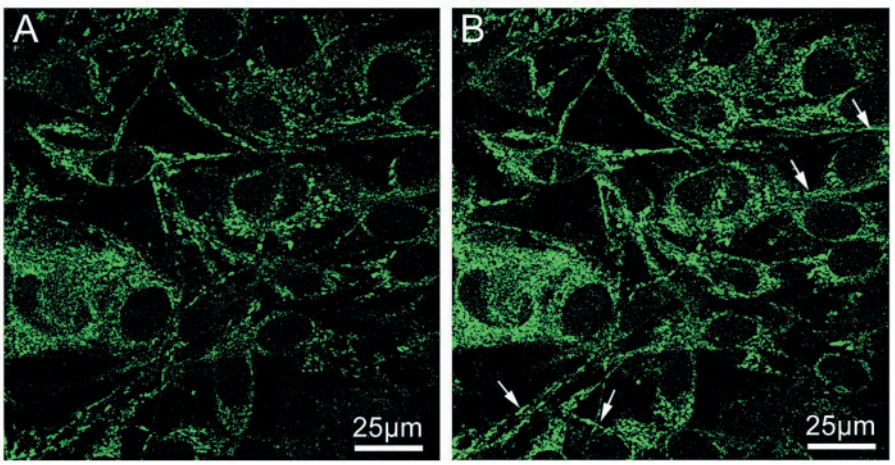


**Fig. 1.** Effects of S1P on F-actin polymerization. C2C12 cells transfected with GFP-tagged α-and β-actin were stimulated with 1 μM S1P under live video two-photon excitation fluorescence microscope. Images were taken at 1 minute (A) and 30 minutes (B) after treatment, respectively. Arrows indicate regions of prominent actin microfilament organization. The images are representative of independent experiments ($n$=12) with similar results.

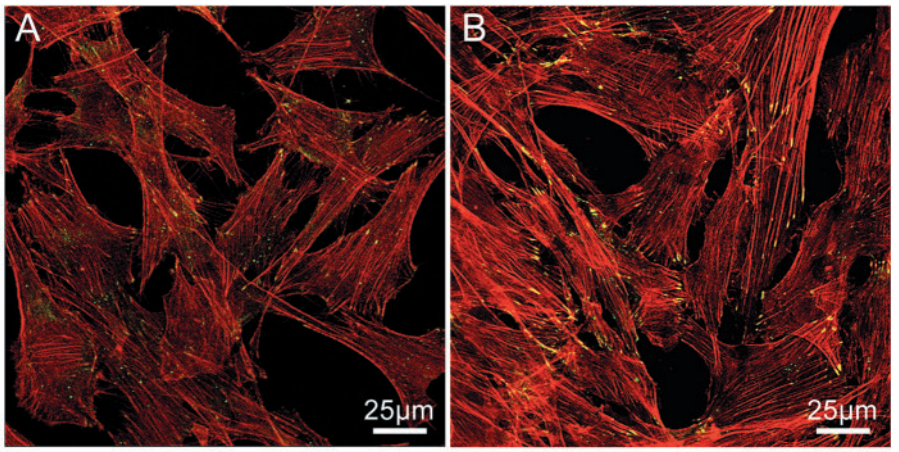


**Fig. 2.** Effects of S1P on stress fibre and focal adhesion formation. Untreated C2C12 myoblasts (A) and treated with 1 μM S1P (B) were fixed and double stained with TRITC-phalloidin (red) and anti-vinculin (green). S1P induces formation of massive stress fibres coincident with the redistribution of vinculin-rich focal adhesion sites at the end of stress fibres. The images are representative of at least three independent experiments with similar results.

mM $MgCl_2$, 10 mM EGTA and 10 mM HEPES, which was filtered through 0.22 μm pores. pH was titrated to 7.4 with NaOH and to 7.2 with TEA-OH for bath and pipette solution, respectively. Patch pipettes were pulled from borosilicate glass (GC 150-15; Clark) using a micropipette puller (Narishige PC-10). When filled, the resistance of the pipettes measured 3-7 MΩ. Experiments were performed on untreated (controls) and C2C12 myoblasts stimulated with S1P (1 μM) for 30 minutes. To ensure that the registered transmembrane currents occurred through putative SACs, parallel experiments were performed using gadolinium chloride ($GdCl_3$; 50 μM; Sigma), which blocks stretch channels, and which was added to control and stimulated myoblasts 3 minutes prior to electrophysiological analysis. The role of F-actin in the regulation of stretch-induced cation fluxes was also assayed by pretreatment with a capping toxin which induced actin filament depolymerization – dihydrocytochalasin B (DHCB; 1 μg/ml; Sigma) – or with DHCB + S1P, which were both added to the culture medium 30 minutes to prior voltage-clamp stimulation. Finally, to provide information on the relationship between the S1P pathway and SAC activity, additional experiments were performed in cells pretreated with the inhibitor of Gi protein PTx, or with the Rho kinase inhibitor Y-27632 and/or transfected with DN-PLD. The patch pipette was connected to a micromanipulator (Narishige International USA) and an Axopatch 200B amplifier (Axon Instruments). Voltage-clamp protocol generation and data acquisition were controlled by using an output and an input of the A/D-D/A interfaces (Digidata 1200; Axon Instruments) and Pclamp 9 software (Axon Instruments). Currents were low-pass filtered at 2 KHz with a Bessel filter and recorded with a sampling interval of 0.1 ms. The cell was held at –60 mV and step pulses, 100 milliseconds of duration, from –80 to 0 mV in 10 mV steps, were applied every 10 seconds. Electrode capacitance was compensated before disrupting the patch. Access resistance ($R_a$) was not compensated for monitoring membrane area. The area beneath the capacitative transient and the time constant of the transient's decay ($\tau$) were used to calculate the cell linear capacitance ($C_m$) and $R_a$ from $\tau = R_a C_m$. The membrane resistance ($R_m$) was calculated from the steady-state membrane current ($I_m$) using the relation: $R_m=(\Delta V - I_m R_a)/I_m$, where $\Delta V$ is the command voltage step amplitude. $C_m$ was measured from $C_m=\Delta Q(R_m+R_a)/R_m\Delta V$, where, to correct for the exponential rise of the voltage step, $\Delta Q$ is the sum of the time integral of the current transient and $I_m\tau$ elicited by each voltage step (Pappone and Lee, 1996). $C_m$ is an index of cell-surface area assuming that membrane-specific capacitance is constant at 1 μF/cm$^2$. To allow comparison of test current recorded from different cells, the $I_m$ amplitude and membrane conductance

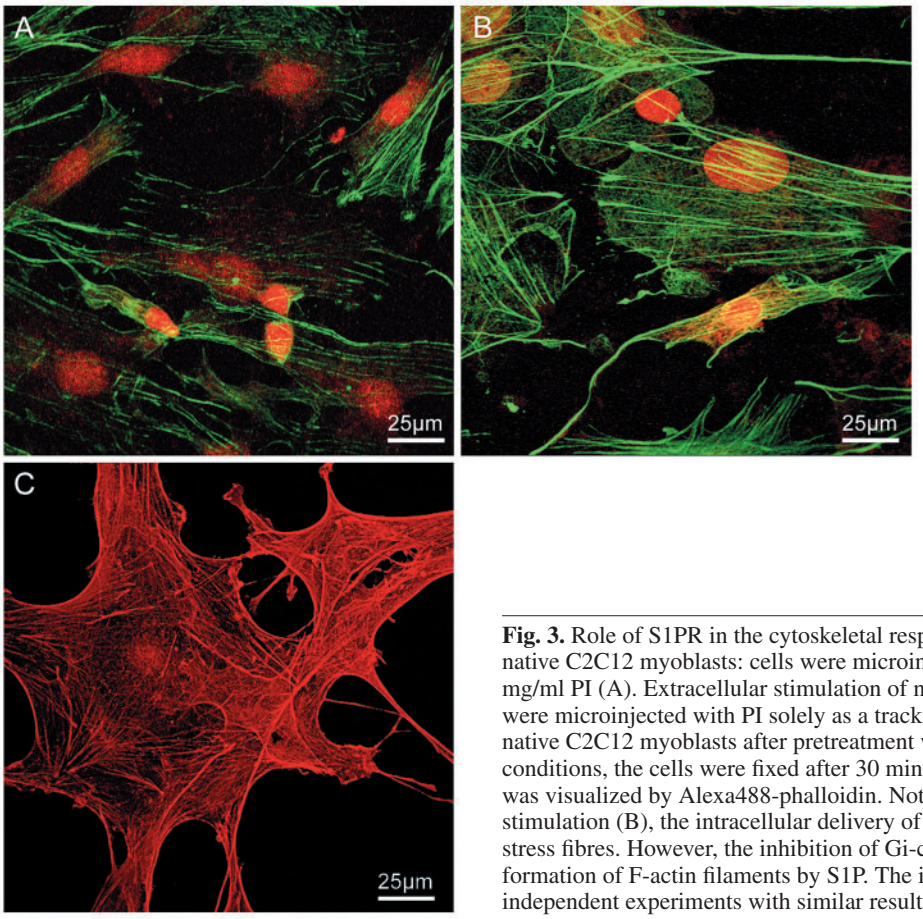


**Fig. 3.** Role of S1PR in the cytoskeletal response of S1P. Intracellular S1P stimulation of native C2C12 myoblasts: cells were microinjected with a mixture of 500 μM S1P and 5 mg/ml PI (A). Extracellular stimulation of native C2C12 myoblasts with 1 μM S1P: cells were microinjected with PI solely as a tracking agent (B). Extracellular stimulation of native C2C12 myoblasts after pretreatment with PTx (C). In all the experimental conditions, the cells were fixed after 30 minutes of stimulation and F-actin organization was visualized by Alexa488-phalloidin. Note that, in contrast to the extracellular stimulation (B), the intracellular delivery of S1P (A) is unable to modify the assembly of stress fibres. However, the inhibition of Gi-coupled receptor pathway by PTx reduces the formation of F-actin filaments by S1P. The images are representative of at least three independent experiments with similar results.

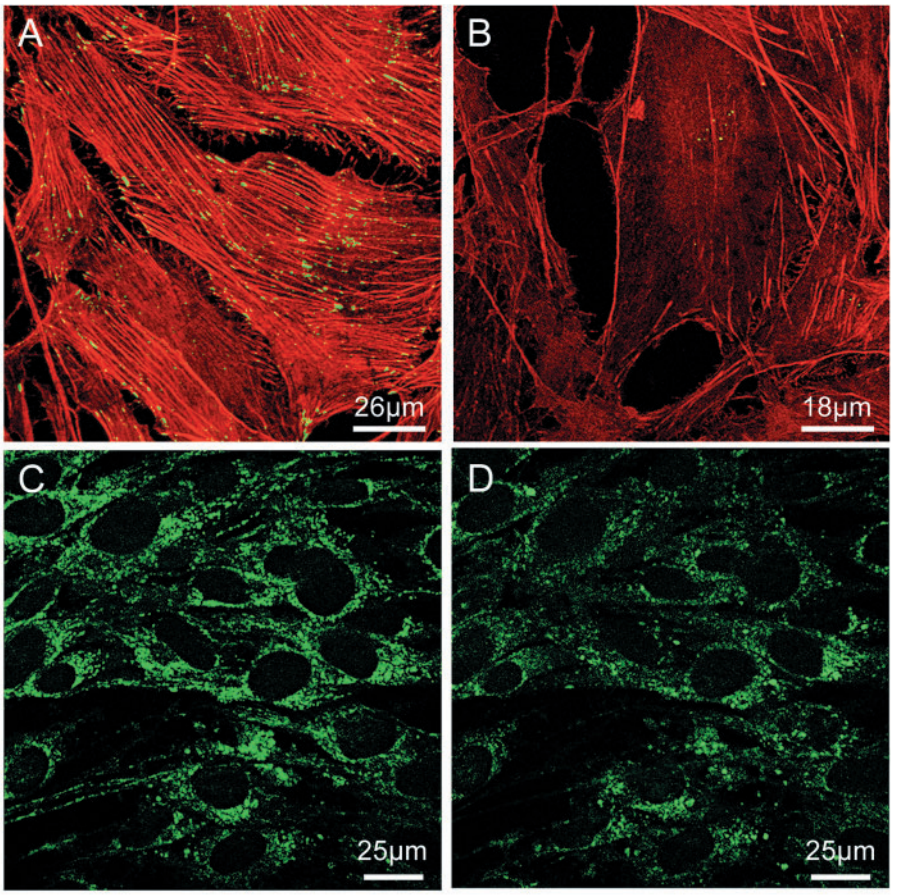


**Fig. 4.** Effects of Rho kinase inhibitor on S1P-induced stress fibres. C2C12 myoblasts were stimulated with 1 μM S1P for 30 minutes in the absence (A) or presence of 50 μM Y-27632 (B), fixed and observed under a confocal laser microscope. Note that, after the pretreatment with the Rho kinase inhibitor, cells have only a few peripheral stress fibres and scattered focal adhesions. Time-lapse analysis of myoblasts expressing GFP-actins by two-photon excitation fluorescence microscopy (C and D). Images were taken 1 minute (C) and 30 minutes after (D) the application of 1 μM S1P. The pretreatment with the Rho kinase inhibitor causes shortening and disruption of actin filaments. The images are representative of at least three independent experiments with similar results.

($G_m$=1/$R_m$) were normalized to $C_m$ (in pA/pF and mS/pF, respectively). All experiments were performed at room temperature (20-23°C). For mathematical and statistical analysis of data, we used pClamp9 (Axon Instruments), SigmaPlot and SigmaStat (Jandel Scientific). Data are as mean±s.e.m. One-way ANOVA with repeated measures was utilized for multiple comparisons and α value at $P$<0.05 was considered significant.

### Mechanical stimulation by atomic force microscopy

To investigate the ability of C2C12 cells to sense mechanical signals, the cells were cultured onto coverslips, pre-loaded with the fluorescent $Ca^{2+}$ dye, Fluo-3 (1 μM; Molecular Probes) and mechanically stimulated using the cantilever of an atomic force microscope (AFM; Pico SPM; Molecular Imaging), according to a previous report (Charras and Horton, 2002). A soft cantilever (0.01 N/mb CSG01; NTMDT; Moscow) was initially positioned in the immediate vicinity of the myoblasts, in contact with the glass surface, then it was laterally moved until reaching the cell surface and finally lifted off the cell. The AFM was mounted on top of an inverted optical microsope (Nikon) equipped with a cooled CCD camera (CHROMA CX 3200; Scientific Instruments). Observations were performed during the mechanical stimulations to ensure that the cells were not

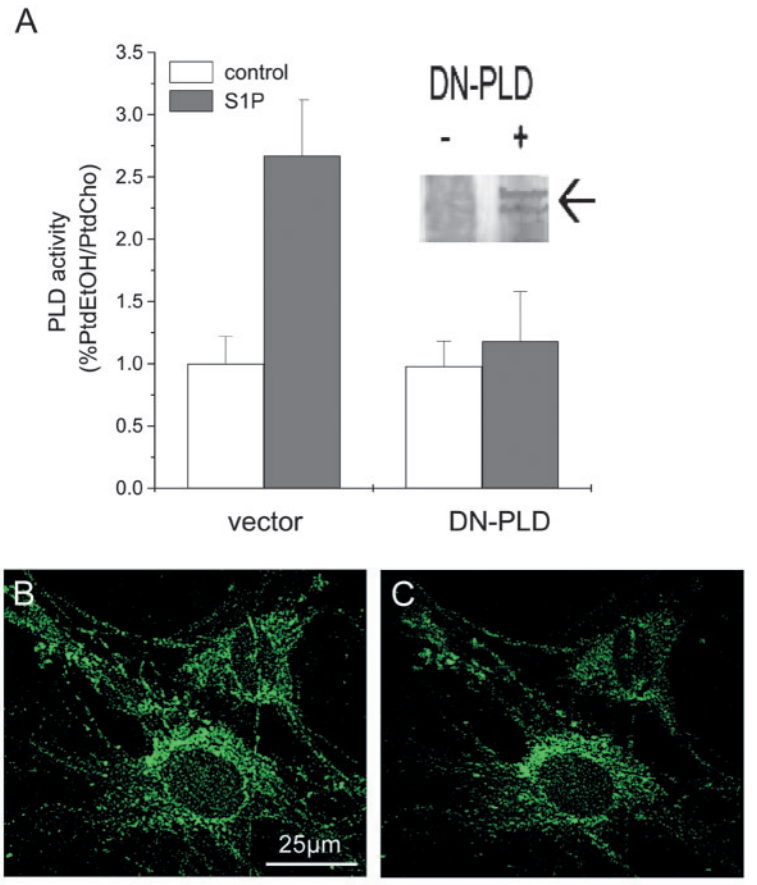


**Fig. 5.** Overexpression of a catalytically inactive PLD mutant affects stress fibre formation. (A) C2C12 cells were transfected with HA-tagged catalytically inactive DN-PLD or empty vector. Following serum starvation, the cells were stimulated with S1P in the presence of ethanol and processed as described in the Materials and Methods. PLD activity is reported as percentage of PtdEtOH on PtdCho. Data are mean±s.e.m. of three independent experiments (*$P$<0.05). Inset: western blot shows the expression of recombinant protein. Blot representative of three experiments with similar results. Time-lapse analysis of myoblasts expressing GFP-actin transfected with DN-PLD by two-photon excitation fluorescence microscopy (B,C). Images were taken 1 minute (B) and 30 minutes after (C) the application of 1 μM S1P. A clear reduction of stress fibres is evident in cells with reduced PLD activity.

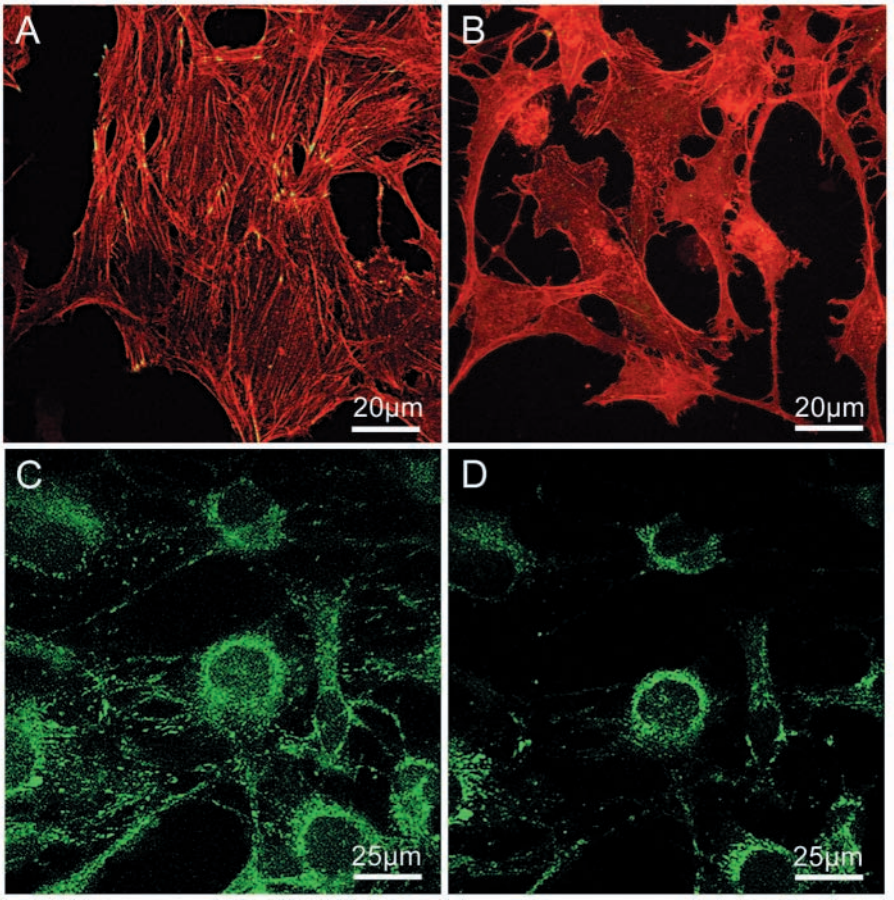


**Fig. 6.** Effects of reduced PLD and Rho kinase activities on S1P-induced stress fibres and focal adhesions. C2C12 myoblasts transfected with DN-PLD were stimulated with 1 μM S1P for 30 minutes (A) or pretreated with 50 μM Y-27632 prior to stimulation (B). The cells were then fixed and double stained with TRITC-phalloidin (red) and anti-vinculin (green). Of interest, the combined treatment is able to abrogate completely stress fibre and focal adhesion formation in response to S1P. (C,D) Time-lapse analysis of C2C12 myoblasts expressing GFP-actins transfected with DN-PLD by two-photon excitation fluorescence microscopy. Images were taken 1 minute (C) and 30 minutes (D) after the application of 1 μM S1P. A complete filament dispersion is visible after 30 minutes from stimulation. The images are representative of at least three independent experiments with similar results.

visibly damaged, as well as after stimulation to visualize intracellular $Ca^{2+}$ transients.

## Results

### Effects of S1P on cytoskeletal reorganization

To visualize actin cytoskeletal dynamics induced by S1P stimulation, we first labelled actin filaments in living myoblasts. According to previous observations showing that myoblasts contain non-muscle contractile proteins (Formigli et al., 2004), the cytoskeletal labelling was performed by transfection of murine α- and β-actin-encoding plasmids into C2C12 myoblasts. Stably transfected C2C12 cells with GFP-tagged actin monomers were then stimulated with 1 μM S1P and observed for up to 1 hour using a multiphoton time-lapse recording system (Fig. 1). The continuous observation showed that, following stimulation, actin monomers underwent dynamic reorganization and were incorporated into F-filaments running across the cell body. This response became visible within 10 minutes, and progressively increased up to 20-30 minutes, then remained practically unmodified thereafter. When fixed and counterstained with TRITC-phalloidin, all the phalloidin-labelled fibres also appeared positive for GFP-labelled α- and β-actin, indicating the successful incorporation of the fusion proteins into the myofilaments (data not shown). Parallel experiments were performed on native C2C12 myoblasts to verify whether increased actin polymerization in response to S1P was associated with stress fibre and focal adhesion formation. The vinculin/F-actin panel in Fig. 2 shows that untreated cells had few, sparse actin filaments and only scattered focal adhesion sites, whereas S1P-stimulated cells exhibited prominent parallel arrays of stress fibres and the polar clustering of vinculin-rich focal adhesions. We next evaluated whether the cytoskeletal effects of S1P were mediated through cell-surface receptors and/or through intracellular targets (Hla, 2003). To this aim, different concentrations (5, 10, 500 μM) of S1P were microinjected into C2C12 cells and their effect on actin filament reorganization was examined. From double fluorescence, used to visualize microinjected cells and stress fibres, it was apparent that intracellular S1P, at all the concentrations used, was unable to influence the assembly of stress fibres in the myoblastic cells (Fig. 3A). By contrast, C2C12 cells microinjected solely with the nuclear dye PI exhibited a remarkable induction of stress fibres in response to the exogenous S1P stimulation (Fig. 3B), suggesting that the S1P-mediated cytoskeletal response was dependent on the binding of the sphingolipid to its specific receptors. Moreover, pretreatment with PTx, to inhibit the Gi-coupled receptor pathway, reduced S1P-induced stress fibre formation, suggesting the contribution of the heterotrimeric G-protein-dependent pathway in this response (Fig. 3C).

### Effects of inhibitors on S1P-induced cytoskeletal reorganization

Since we have previously shown that activation of S1PRs induces contraction of Rho-dependent myoblastic cells (Formigli et al., 2004), and in consideration of the suggested role played by acto-myosin interactions in stress fibre formation and maintenance (Chrzanowska-Wodnicka and Burridge, 1996), we examined whether Rho/Rho kinase cascade was involved in S1P-induced C2C12 cytoskeletal reorganization. Inactivation of the Rho effector, Rho Kinase, by Y-27632 (50 μM) greatly interfered with the formation of

stress fibres and focal adhesions in S1P-stimulated cells, causing a dramatic reduction in the number of stress fibres (Fig. 4A,B). When the pretreatment was performed in living GFP-actin-expressing cells, the inhibitory effect on stress fibre formation was associated with the disassembly of pre-existing actin filaments (Fig. 4C,D).

We next explored whether PLD activation could also play a role in mediating the S1P effects on the myoblastic cytoskeleton. Owing to the high susceptibility of C2C12 cells to the pretreatment with alcohols, such as butan-1-ol, the reduction of PLD activity was performed by the transient overexpression of an inactive PLD1 mutant (DN-PLD). PLD activity was assayed in vivo by the measurement of the formation of phosphatidylethanol. In cells overexpressing DN-PLD, S1P failed to increase PLD activity (Fig. 5), indicating that PLD1 contributed significantly to the total cellular PLD activity in C2C12 cells. Expression of DN-PLD was confirmed by western blot using antibodies against the HA epitope (shown in Fig. 5 inset). Moreover, the reduction of endogenous PLD activity caused a selective thinning of stress fibres in response to S1P, in both the wild-type C2C12 cells and GFP-actin-expressing C2C12 cells (Fig. 5B,C) However, this effect was less evident than that exerted by inhibition of Rho kinase activity. Consistent with the efficiency of transient transfection (assessed around 40%), not all the stimulated cells showed decreased actin cytoskeleton and some of them formed robust stress fibres. Finally, the treatment with Y27632 of the cells overexpressing DN-PLD completely abrogated the S1P-induced effects and concomitantly altered the cell shape in both the wild-type and GFP-actin-expressing myoblasts (Fig. 6B,C,D), suggesting that S1P-mediated cytoskeletal rearrangement depended on the Rho/Rho kinase and PLD activities. According to these data, in parallel experiments we also found that S1P-induced stress fibre formation and focal adhesions were independent from the activity of p38 MAP kinase and ERK1/2, because these effects were not perturbed by the use of the specific inhibitors SB203580 (5 μM) and PD98059 (5 μM), respectively (data not shown).

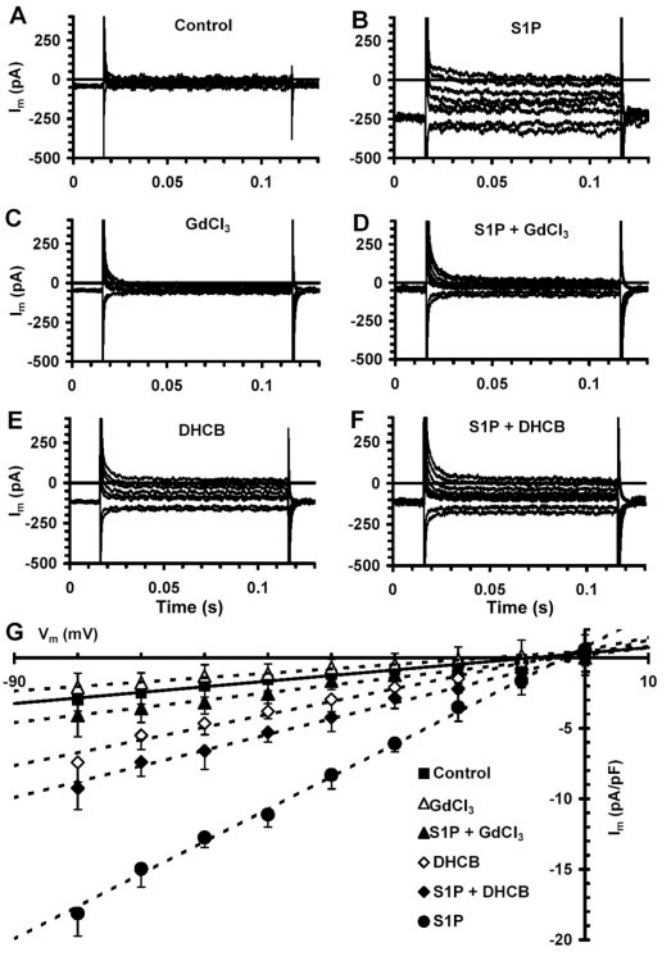


**Fig. 7.** Effects of S1P and of chemical treatments on membrane current and conductance. Voltage-clamp step pulses between –80 and 0 mV in 10 mV steps from a holding potential of –60 mV were applied to the cells for 100 milliseconds. Representative current traces in control (A) and after S1P (B), $GdCl_3$ (C), S1P + $GdCl_3$ (D), DHCB (E) and S1P + DHCB (F) treatments. G, normalized $I_m$ versus Vm plots in Control condition (■) and after S1P (●) or $GdCl_3$ (△) or S1P + $GdCl_3$ (▲) or DHCB(◇) or S1P + DHCB(◆) treatment. The best linear regression lines are superimposed on control (continuous line) and the other experimental conditions (dashed lines). The calculated $C_m$, $G_m$ and $G_m/C_m$ values for all experimental conditions are reported in Table 1. Data are the mean±s.e.m.

## Electrophysiological analysis

We next sought to determine the possible physiological implications of the S1P-induced cytoskeletal remodelling. Since there is a direct link between the cytoskeletal network and SACs (Glogauer et al., 1998), we investigated the role played by S1P-induced stress fibres in modulating channel activity. To this purpose, we performed electrophysiological recordings of plasma membrane currents in single C2C12 myoblasts using the conventional whole-cell voltage-clamp method with a physiological salt solution in the bath and a high-[$Cs^+$] solution in the pipette. The resting membrane potential recorded in current-clamp was highly variable in control cells, ranging between –40 and –20 mV. Voltage-clamp

**Table 1. Plasma membrane properties in control conditions and after chemical treatments**

| | Control (18) | S1P (14) | $GdCl_3$ (8) | S1P + $GdCl_3$ (10) | DHCB (8) | S1P + DHCB (10) |
|---|---|---|---|---|---|---|
| $C_m$ (pF) | 20.1±1.9 | 19.1±2.3 | 21.5±1.8 | 19.5±2.4 | 23.6±2.4 | 22.7±2.6 |
| $G_m$ (nS) | 0.7±0.4 | 4.4±1.1** | 0.7±0.4 | 0.8±0.4 | 2.1±0.7* | 2.7±0.8* |
| $G_m/C_m$ (mS/pF) | 36.7±6.7 | 230.1±30.4** | 34.7±5.8 | 42.7±8.4 | 90.5±25.5* | 118.1±36.4* |

Cell membrane capacitance ($C_m$), conductance ($G_m$) and $G_m/C_m$ of myoblasts in control condition and after treatment with S1P, $GdCl_3$, S1P + $GdCl_3$, DHCB, or S1P + DHCB.

* and ** indicate parameters that are statistically different at $P<0.01$ and $P<0.005$, respectively, from those in Control condition. No parameters of S1P + DHCB are statistically different ($P<0.05$) from those of DHCB. Data were analysed using one-way ANOVA with the Bonferroni's correction for multiple comparisons. Data are the mean±s.e.m. The number of myoblasts investigated is reported in brackets.

**Table 2. Plasma membrane properties after inhibition of Rho, PLD and Gi-dependent functions**

| | Vector (5) | DN-PLD (8) | Y-27632 (8) | DN-PLD + Y-27632 (6) | PTx (11) |
|---|---|---|---|---|---|
| $C_m$ (pF) | 20.6±2.8 | 21.1±2.5 | 19.6±2.5 | 19.9±2.5 | 20.5±2.8 |
| $G_m$ (nS) | 4.6±1.3 | 3.2±1.2* | 0.9±0.7*** | 0.8±0.9*** | 1.4±0.8** |
| $G_m/C_m$ (mS/pF) | 223.0±30.8 | 151.7±32.8* | 45.9±7.9*** | 38.2±15.8*** | 68.2±18.8** |

$C_m$, $G_m$ and $G_m/C_m$ of S1P-stimulated myoblasts after transfection with the empty Vector, transfection with DN-PLD, pretreatment with Y-27632 (50 μM), transfection with DN-PLD + Y-27632, or pretreatment with PTx (200 ng/ml). *, ** and *** indicate parameters that are statistically different at $P<0.01$, $P<0.005$ and $P<0.001$, respectively, from those reported in Table 1, S1P column. Data were analysed using one-way ANOVA with the Bonferroni's correction for multiple comparisons. Data are the mean±s.e.m. The number of myoblasts investigated is reported in brackets.

step pulses between –80 and 0 mV, in 10 mV steps from a holding potential of –60 mV, were applied to the cells for 100 milliseconds. The current trace recordings from controls and treated myoblasts are shown in Fig. 7A-F, whereas the values of the membrane capacitance ($C_m$), conductance ($G_m$) and $G_m/C_m$ of all the examined myoblasts are reported in Table 1. Finally, the recorded steady-state $I_m$ normalized to $C_m$ plotted as a function of the membrane potential ($V_m$) is reported in Fig. 7G. The current traces and $I_m$ versus $V_m$ plots showed that, compared with control myoblasts (Fig. 7A, G ■), myoblasts stimulated with S1P (1 μM) had higher (5/6-fold increase) basal $I_m$ (Fig. 7B, G ●). To verify the involvement of SA channels in this response, we examined the effects of $GdCl_3$, a well-known blocker of these channels. Unstimulated (controls) and stimulated C2C12 cells were incubated with 5 μM $GdCl_3$ (3 minutes) and subjected to the same experimental pulse protocol. It was found that the pretreatment with $GdCl_3$ suppressed $I_m$ in S1P-stimulated myoblasts (Fig. 7D, G ▲), whereas it did not affect that of control myoblasts (Fig. 7C, G △). We also examined whether F-actin could act as a mechanotransducer in our model, influencing the openings of SACs. To this purpose, the cells were incubated for 30 minutes with DHCB, a drug that inhibits actin polymerization, prior to stimulation. However, before performing the electrophysiological measurements, we tested whether this reagent actually depolymerized F-actin. Staining with phalloidin showed that the treatment with DHCB completely disrupted the actin network in both the control and S1P-stimulated myoblasts (data not shown). The application of DHCB (1 μg/ml) in unstimulated C2C12 cells caused a slight but significant increase in $I_m$ compared with that of controls (Fig. 7E, G ◇); however, it led to a marked decrease in $I_m$ in S1P-stimulated myoblasts (Fig. 7F, G ◆), suggesting that the cytoskeleton integrity could play a pivotal role in modulating the plasma membrane tension and, in turn, SAC activity. The statistical analysis of the data further confirmed the role of non-selective cation SACs in mediating the electrical response of myoblasts to S1P stimulation. The $I_m$ versus $V_m$ relationship was, in fact, linear over all the membrane potential examined and the reversal potentials ($V_{rev}$) were between –5 and 0 mV (Fig. 7G), thus excluding the involvement of currents through voltage-dependent, anionic SA (Cl-selective) and $Ca^{2+}$-selective ion channels (Setoguchi et al., 1997).

To examine the relationship between S1P signalling and SAC activation, additional experiments were performed in C2C12 cells with impaired Rho kinase and PLD functions. We found that: (1) pretreatment with the Rho kinase inhibitor Y-27362 (50 μM) reduced by approximately 80% the increase in $I_m$ and $G_m/C_m$ in response to S1P stimulation (Fig. 8C, F ○; Table 2); (2) transient transfection with DN-PLD caused 34% reduction in $I_m$ and $G_m/C_m$ (Fig. 8B, F ▲; Table 2), whereas transfection of the cells with the empty vector did not have any effects on the electrical parameters (Fig. 8F ●; Table 2); (3) the combined treatments completely blocked the effects of S1P on SAC regulation (Fig. 8D, F △; Table 2); and (4) pretreatment with PTx reduced by approximately 70% the S1P-induced increases in $I_m$ and $G_m/C_m$ (Fig. 8E, F ◇; Table 2), suggesting that activation of the Gi-coupled receptor was required for the modulation of SACs by S1P.

### Mechanically evoked calcium transients

To assess the effects of membrane stretching on the modulation of stretch-activated $Ca^{2+}$ influx, C2C12 cells were loaded with the $Ca^{2+}$ indicator Fluo-3 and mechanically stimulated with the cantilever of an AFM. After stretching, a rapid increase in the intracellular $Ca^{2+}$ was observed in most of the stimulated cells, as indicated by an increase in the fluorescence intensity. The increase in intracellular $Ca^{2+}$ was detected as soon as the cantilever touched the plasma membrane (Fig. 9); this event was followed by the intercellular propagation of $Ca^{2+}$ transients to neighbouring cells, owing to the presence of functional gap junctions at the sites of cell-to-cell contacts among the myoblastic cells (Formigli et al., 2005).

## Discussion

Data presented in this study extend our previous observations on the effects of S1P on the myoblastic cell functions. We have demonstrated that S1P, besides activating cell contraction and increasing intracellular $Ca^{2+}$ (Formigli et al., 2002; Meacci et al., 2002), is also able to regulate actin cytoskeleton reorganization by stimulating stress fibre and focal adhesion formation in C2C12 cells. In such a view, the present data are consistent with the well-established role of S1P and of its structurally and functionally related lysophospholipid, lysophosphatidic acid, in the modulation of actin-mediated functions, including cell contraction, cell adhesion and migration (Rosenfeldt et al., 2003; Shikata et al., 2003a). In particular, live videoimaging of GFP-α-actin- and GFP-β-actin-expressing C2C12 myoblasts showed that the stimulation with S1P caused de novo actin polymerization with a concomitant clustering of pre-existing F-actin filaments, suggesting that the myoblastic cytoskeleton represented an important cellular target for S1P action. The intracellular delivery of S1P by microinjection was unable to induce actin reorganization, suggesting the involvement of high-affinity S1P cell-surface receptors in this response. These findings are in agreement with previous reports (Wang et al., 1997; Olivera

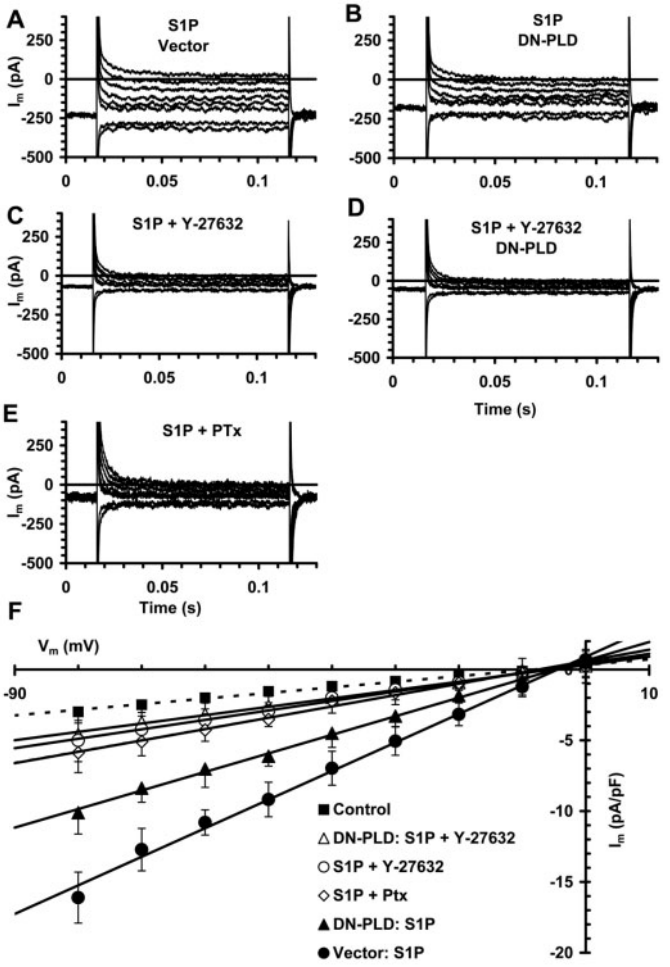


**Fig. 8.** Effects of S1P and of the inhibition of Rho kinase, PLD and Gi-coupled receptor on membrane current and conductance. (A-E) Voltage-clamp step pulses as in Fig. 7. Representative current traces (A-E) and normalized $I_m$ versus $V_m$ plots (F) after S1P stimulation in: empty vector transfected myoblast (A, ● in F); DN-PLD-transfected myoblasts (B, ▲ in F); Y-27362-treated myoblasts (C, ○ in F); DN-PLD-transfected myoblasts in the presence of Y-27362 (D, △ in F); PTx-treated myoblasts (A, ◇ in F). The best linear regression lines are superimposed on the data (continuous lines). For comparison, the data and linear regression (dashed line) of control from Fig. 7 are reported. The calculated $C_m$, $G_m$ and $G_m/C_m$ values for all experimental conditions are reported in Table 2. Data are the mean±s.e.m.

et al., 2003), and are consistent with our recent results showing that the downregulation of S1PRs by antisense oligodeoxyribonucleotides strongly attenuated S1P-induced actin dynamics in C2C12 myoblasts (E.M., unpublished observations). The detailed analysis of the target molecules involved in the pathway linking S1PR activation to the cytoskeletal effects showed that Rho/Rho kinase and PLD activities were both required for stress fibre formation. In fact, defects in the formation of stress fibres were observed after pretreatment with the Rho kinase inhibitor Y-27632, or in myoblasts in which PLD activity could not be increased by S1P. Moreover, the combined treatment resulted in a total inhibition of S1P-induced cytoskeletal response. The inhibition studies also showed that stress fibres were more sensitive to the impairment of Rho kinase than of PLD. These data are consistent with growing evidence suggesting that Rho kinase pathway plays a key role in the regulation of the actin cytoskeleton (Chrzanowska-Wodnicka and Burridge, 1996), and with our previous observations that stimulation with S1P increases the levels of myosin light chain phosphorylation (Formigli et al., 2004). In fact, it has been proposed that phosphorylation of myosin light chain phosphatase by Rho kinase decreases phosphatase activity, thereby increasing the level of phosphorylated myosin light chains that bind to actin. The contractile tension exerted by myofilament interaction, in turn, is thought to induce F-actin bundling into stress fibre and focal adhesion aggregation (Burridge et al., 1997; Ridley, 2001). Further clues to this effect came from the present data showing that pretreatment with Y-27632 caused substantial dispersion of filaments in both control and S1P-treated GFP-actin-expressing cells, probably decreasing the basal levels of myosin light chain phosphorylation. It is also likely that other Rho effector pathways, including mDia and ERM proteins, might contribute to the cytoskeletal response to S1P by favouring accumulation of polymerized actin (Sah et al., 2000). The role of PLD activation in actin rearrangement by S1P is in agreement with our previous observations that S1P elicits PLD activation in the C2C12 myoblasts (Meacci et al., 1999a) and with the requirement for Rho in the regulation of PLD activity by S1P (Meacci et al., 2001). Moreover, previous studies have reported the involvement of PLD in S1P- and lysophosphatidic acid-induced stress fibre formation in other cell types (Porcelli et al., 2002). However, contrary to the well-established Rho

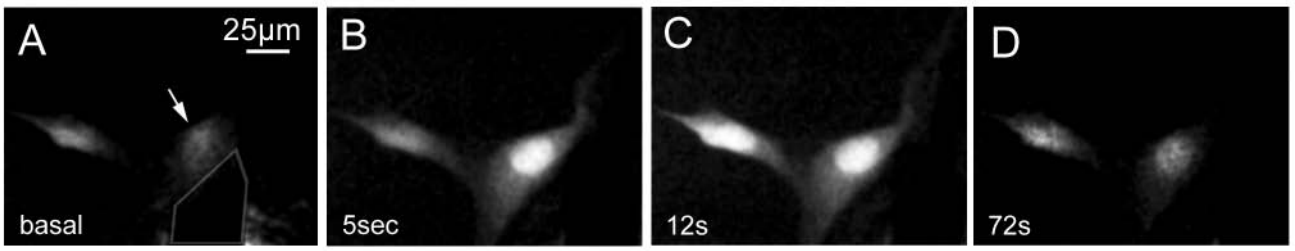


**Fig. 9.** $Ca^{2+}$ influx after the application of stretching forces. Native C2C12 cells were pre-loaded with Fluo-3 (1 μM) and mechanically stimulated using the cantilever (white line) of an AFM. Arrow points to the cell to be stretched. The images were recorded by a cooled CCD camera prior and after the cantilever had been lifted off the cell at the indicated time points. The myoblast responds to the mechanical stimulus by a rise in intracellular $Ca^{2+}$ that propagates from the stretched cell to the adjacent one. The images are representative of at least three independent experiments with similar results.

functions, the molecular targets of PLD activation are still poorly understood. A role for phosphatidic acid formed by S1P-induced PLD activity as a modulator of targets distinct from the Rho pathway is worthy of further investigation.

Stress fibre and focal adhesion formation promoted by S1P in myoblastic cells may have relevant physiological implications. In particular, actin filaments have been described to modulate SACs (Glogauer et al., 1998; Wu et al., 1999) and modifications of the basal channel activity have been reported after disruption of actin filaments with DHCB (Nakamura et al., 2001). Interestingly, in the present study, we have shown that pretreatment with DHCB caused a small, but significant, increase in the ion conductance through the mechanosensitive ion channels, thus further supporting the role played by the intact cytoskeleton in the regulation of channel sensitivity. However, on the basis of the current knowledge that cells use tensegrity architecture for their organization and mechanotrasduction (Ingber, 2003), it may be argued that organized actin filaments might exert, to the same extent as actin depolymerization, tension forces at the plasma membrane and, in turn, promote the opening of SACs. In this connection, we provided novel experimental evidence that stress fibre and focal adhesion formation in response to S1P provoked an increase in the ion currents through SACs. Indeed, the whole-cell patch-clamp analysis showed that both normalized $I_m$ and $G_m$ were strongly inhibited in the following experimental conditions: (1) after application of the SAC blocker $GdCl_3$ and of the actin-depolymerizing agent DHCB; and (2) after pretreatment with the Rho kinase inhibitor Y-27632, and in cells with reduced endogenous PLD activity. From these results, it is proposed that S1P might exert a modulatory effect on SACs through stimulation of stress fibre and focal adhesion formation. Interestingly, we also found that inactivation of Gi-dependent signalling by PTx also seriously affected the increased ion current and conductance through SACs. These findings are in agreement with our previous observations that PLD activation in myoblasts occurs through Gi-coupled receptor mechanisms (Meacci et al., 1999a), and suggest novel mechanisms of SAC modulation. Given that PLD activation alters cortical actin dynamics (Colley et al., 1997; Platek et al., 2004), it may be speculated that PLD-dependent pathways play a pivotal role in regulating SAC activity by not only contributing to stress fibre formation but also by affecting the peripheral cytoskeletal assembly, which is probably necessary for transducing the mechanical tension to the plasma membrane. Experiments are ongoing in our laboratory to test this hyphothesis.

Finally, experiments aimed at stretching the plasma membrane using the cantilever of an AFM indicated that there was a $Ca^{2+}$ influx through putative SACs. In such a view, and in consideration that $Ca^{2+}$ is an important second messenger for skeletal muscle differentiation (Konig et al., 2004), it may be suggested that the formation of a well-organized cytoskeleton and the correlated increase in SAC permeability in response to S1P might represent a potential mechanism by which the bioactive lipid affects skeletal muscle differentiation. In agreement, S1P has been implicated in differentiation processes of various cell types (Pyne and Pyne, 2000) and preliminary results are in favour of a role of the sphingolipid in myogenic differentiation (E.M., unpublished observations).

In conclusion, in this study, we report that S1P promotes the formation of stress fibres and focal adhesions in C2C12 myoblasts and that this response depends on the activation of the Rho and PLD cascades. Interestingly, there was a strong correlation between S1P-induced actin cytoskeletal reorganization and increased plasma membrane ion currents and $Ca^{2+}$ influx through SACs. We propose that Rho/PLD signalling, and cytoskeleton and SAC activation may be partners in the differentiative response of myoblasts to S1P.

This paper was supported by grants from the Italian Ministery for University (Cofin 2003) to S.Z.-O., P.B. and F.F.; from the University of Florence (ex. 60%) to L.F., S.Z.-O., F.F. and P.B.; and from Ente Cassa di Risparmio di Firenze to P.B. We gratefully acknowledge the image-processing by D. Nosi.

## References

**Arai, A., Spencer, J. A. and Olson, E. N.** (2002). STARS, a striated muscle activator of Rho signaling and serum response factor-dependent transcription. *J. Biol. Chem.* **277**, 24453-24459.

**Berridge, M. J., Lipp, P. and Bootman, M. D.** (2000). The versatility and universality of calcium signalling. *Nat. Rev. Mol. Cell. Biol*. 1, 11-21.

**Burridge, K., Chrzanowska-Wodnicka, M. and Zhong, C.** (1997). Focal adhesion assembly. *Trends Cell. Biol.* **7**, 342-347.

**Charras, G. T. and Horton, M. A.** (2002). Single cell mechanotransduction and its modulation analyzed by atomic force microscope indentation. *Biophys. J.* **82**, 2970-2981.

**Chrzanowska-Wodnicka, M. and Burridge, K.** (1996). Rho-stimulated contractility drives the formation of stress fibers and focal adhesions. *J. Cell Biol.* **133**, 1403-1415.

**Colley, W. C., Sung, T. C., Roll, R., Jenco, J., Hammond, S. M., Altshuller, Y., Bar-Sagi, D., Morris, A. J. and Frohman, M. A.** (1997). Phospholipase D2, a distinct phospholipase D isoform with novel regulatory properties that provokes cytoskeletal reorganization. *Curr. Biol*. **7**, 191-201.

**Denk, W., Strickler, J. H. and Webb, W. W.** (1990). Two-photon laser scanning fluorescence microscopy. *Science* **248**, 73-76.

**Formigli, L., Francini, F., Meacci, E., Vassalli, M., Nosi, D., Quercioli, F., Tiriblli, B., Bencini, C., Piperio, C., Bruni, P. et al.** (2002). Sphingosine 1-phosphate induces $Ca^{2+}$ transients and cytoskeletal rearrangement in $C_2C_{12}$ myoblastic cells. *Am. J. Physiol. Cell. Physiol.* **282**, C1361-C1373.

**Formigli, L., Meacci, E., Vassalli, M., Nosi, D., Quercioli, F., Tiribilli, B., Tani, A., Squecco, R., Francini, F., Bruni, P. et al.** (2004). Sphingosine 1-phosphate induces cell contraction via calcium-independent/Rho dependent pathways in undifferentiated skeletal muscle cells. *J. Cell Physiol*. **198**, 1-11.

**Formigli, L., Francini, F., Tani, A., Squecco, R., Nosi, D., Polidori, L., Nistri, S., Chiappini, L., Cesati, V., Pacini, A., Perna, A. M., Orlandini, G. E., Zecchi-Orlandini, S. and Bani, D.** (2005). Morphofunctional integration between skeletal myoblasts and adult cardiomyocytes in coculture is favored by direct cell-cell contacts and relaxin treatment. *Am. J. Physiol. Cell Physiol.* doi:10.1152/ajpcell.00345.

**Glogauer, M., Arora, P., Chou, D., Janmey, P. A., Downey, G. P. and McCulloch, C. A. G.** (1998). The role of actin-binding protein 280 in integrin-dependent mechanoprotection. *J. Biol. Chem.* **16**, 1689-1698.

**Hall, A.** (1998). Rho GTPases and the actin cytoskeleton. *Science* **279**, 509-514.

**Hla, T.** (2003). Signaling and biological actions of sphingosine 1-phosphate. *Pharmacol. Res.* **47**, 401-407.

**Hodgson, L., Qiu, W., Dong, C. and Henderson, A. J.** (2000). Use of green fluorescent protein-conjugated β-actin as a novel molecular marker for in vitro tumor cell chemotaxis assay. *Biotechnol. Prog*. **16**, 1106-1114.

**Hubchack, S. C., Runyan, C. E., Kreisberg, J. I. and Schnaper, H. W.** (2003). Cytoskeletal rearrangement and signal transduction in TGF-beta 1-stimulated mesangial cell collagen accumulation. *J. Am. Soc. Nephrol.* **14**, 1969-1980.

**Ingber, D. E.** (2003). Tensegrity I. Cell structure and hierarchical systems biology. *J. Cell Sci.* **116**, 1157-1173.

**Kam, Y. and Exton, J. H.** (2001). Phospholipase D activity is required for actin stress fiber formation in fibroblasts. *Mol. Cell. Biol.* **21**, 4055-4066.

**Konig, S., Hinard, V., Arnaudean, S., Holzer, N., Potter, G., Bader, C. R. and Bernheim, L.** (2004). Membrane hyporpolarization triggers myogenin

and myocyte enhancer factor-2 expression during human myoblast differentiation. *J. Biol. Chem.* **279**, 28187-28196.

**Mack, C. P., Somlyo, A. V., Hautmann, M., Somlyo, A. P. and Owens, G. K.** (2001). Smooth muscle differentiation marker gene expression is regulated by RhoA-mediated actin polymerization. *J. Biol. Chem.* **276**, 341-347.

**Meacci, E., Vasta, V., Donati, C., Farnararo, M. and Bruni, P.** (1999a). Receptor-mediated activation of phospholipase D by sphingosine 1-phosphate in skeletal muscle C2C12 cells. A role for protein kinase C. *FEBS Lett.* **27**, 184-188.

**Meacci, E., Vasta, V., Moorman, J. P., Bobak, D. A., Bruni, P., Moss, J. and Vaughan, M.** (1999b). Effect of Rho and ADP-ribosylation factor GTPases on phospholipase D activity in intact human adenocarcinoma A549 cells. *J. Biol. Chem.* **274**, 18605-18612.

**Meacci, E., Donati, C., Cencetti, F., Komuro, I., Farnararo, M. and Bruni, P.** (2001). Dual regulation of sphingosine 1-phosphate-induced phospholipase D activity through Rho A and ptotein kinase Cα in C2C12 myoblasts. *Cell Signal*. **13**, 593-598.

**Meacci, E., Cencetti, F., Formigli, L., Squecco, R., Donati, C., Tiribilli, B., Quercioli, F., Zecchi Orlandini, S., Francini, F. and Bruni, P.** (2002). Sphingosine 1-phosphate evokes calcium signals in C2C12 myoblasts via Edg3 and Edg5 receptors. *Biochem. J.* **362**, 349-357.

**Munevar, S., Wang, Y. and Dembo, M.** (2004). Regulation of mechanical interactions between fibroblasts and the substratum by stretch-activated $Ca^{2+}$ entry. *J. Cell Sci*. **117**, 85-92.

**Nakamura, T. Y., Iwata, Y., Sampaolesi, M., Hanada, H., Saito, N., Artman, M., Coetzee, W. A. and Shigekawa, M.** (2001). Stretch-activated cation channels in skeletal muscle myotubes from sarcoglycan-deficient hamsters. *Am. J. Physiol. Cell. Physiol*. **281**, C690-C699.

**Olivera, A., Rosenfeldt, H. M., Bektas, M., Wang, F., Ishii, I., Chun, J., Milstien, S. and Spiegel, S.** (2003). Sphingosine kinase type 1 induces $G_{12/13}$-mediated stress fiber formation, yet promotes growth and survival independent of G protein-coupled receptors. *J. Biol. Chem.* **278**, 46452-46460.

**Panetti, S., T., Magnusson, M. K., Peyruchaud, O., Zhang, Q., Cooke, M. E., Sakai, T. and Mosher, D. F.** (2001). Modulation of cell interactions with extracellular matrix by lysophosphatidic acid and sphingosine 1-phosphate. *Prostaglandins* **64**, 93-106.

**Pappone, P. A. and Lee, S. C.** (1996). Purinergic receptor stimulation increase membrane trafficking in brown adipocytes. *J. Gen. Physiol*. **108**, 393-404.

**Platek, A., Mettlen, M., Camby, I., Kiss, R., Amyere, M. and Courtoy, P. J.** (2004). v-Src accelerates spontaneous motility via phosphoinositide 3-kinase, phospholipase C and phospholipase D, but abrogates chemotaxis in Rat-1 and MDCK cells. *J. Cell Sci.* **117**, 4849-4861.

**Porcelli, A. M., Ghelli, A., Hrelia, S. and Rugolo, M.** (2002). Phospholipase D stimulation is required for sphingosine 1-phosphate activation of actin stress fibre assembly in human epithelial cells. *Cell Signal*. **14**, 75-81.

**Pyne, S. and Pyne, N. J.** (2000). Sphingosine 1-phosphate signalling in mammalian cells. *Biochem. J.* **349**, 385-402.

**Quercioli, F., Ghirelli, A., Tiribilli, B. and Vassalli, M.** (2004). Ultracompact autocorrelator for multiphoton microscopy. *Microsc. Res. Tech.* **63**, 27-33.

**Ridley, A. J.** (2001). Rho family proteins: coordinating cell responses. *Trends Cell Biol.* **11**, 471-477.

**Rosenfeldt, H. M., Amrani, Y., Watterson, K. R., Murthy, K. S., Panettieri, R. A., Jr and Spiegel, S.** (2003). Sphingosine-1-phosphate stimulates contraction of human airway smooth muscle cells. *FASEB J.* **17**, 789-799.

**Sah, V. P., Seasholtz, T. M., Sagi, S. A. and Brown, J. H.** (2000). The role of Rho in G protein-coupled receptor signal transduction. *Annu. Rev. Pharmacol. Toxicol.* **40**, 459-489.

**Seasholtz, T. M., Majumdar, M. and Brown, J. H.** (1999). Rho as a mediator of G protein-coupled receptor signaling. *Mol. Pharmacol.* **55**, 949-956.

**Setoguchi, M., Ohya, Y., Abe, I. and Fujishima, M.** (1997). Stretch-activated whole-cell currents in smooth muscle cells from mesenteric resistance artery of guinea-pig. *J. Physiol*. **501**, 343-353.

**Shikata, J., Birukov, K. G., Birukova, A. A., Verin, A. and Garcia, J. G. N.** (2003a). Involvement of site-specific FAK phosphorylation in sphingosine-1 phosphate and thrombin-induced focal adhesion remodeling: role of Src and GIT. *FASEB J.* **17**, 2240-2249.

**Shikata, Y., Birukov, K. G. and Garcia, J. G. N.** (2003b). S1P induces FA remodeling in human pulmonary endothelial cells: role of Rac, GIT1, FAK and paxillin. *J. Appl. Physiol.* **94**, 1193-1203.

**Sotiropoulos, A., Gineitis, D., Copeland, J. and Treisman, R.** (1999). Signal-regulated activation of serum response factor is mediated by changes in actin dynamics. *Cell* **98**, 159-169.

**Takano, H., Komuro, I., Oka, T., Shiojima, I., Hiroi, Y., Mizuno, T. and Yazaki, Y.** (1998). The Rho family G proteins play a critical role in muscle differentiation. *Mol. Cell. Biol*. **18**, 1580-1589.

**Turner, C. E.** (2000). Paxillin and focal adhesion signalling. *Nat. Cell Biol.* **2**, E231-E236.

**Van Aelst, L. and D'Souza-Schorey, C.** (1997). Rho GTPases and signaling networks. *Genes Dev*. **11**, 2295-2322.

**Wang, F., Nobes, C. D., Hall, A. and Spiegel, S.** (1997). Sphingosine 1-phosphate stimulates Rho-mediated tyrosine phosphorylation of focal adhesion kinase and paxillin in Swiss 3T3 fibroblasts. *Biochem. J.* **324**, 481-488.

**Wu, Z., Wong, K., Glogauer, M., Ellen, P. R. and McCulloch, C. A. G.** (1999). Regulation of stretch-activated intracellular calcium transients by actin filaments. *Biochem. Biophys. Res. Commun*. **261**, 419-425.